Article

DNA Polymorphism as an Origin of Adenine-Thymine Tract Length-Dependent Threading Intercalation Rate

Pa#r Nordell, Fredrik Westerlund, Anna Reymer, Afaf H. El-Sagheer, Tom Brown, Bengt Norde#n, and Per Lincoln

J. Am. Chem. Soc., **2008**, 130 (44), 14651-14658 • DOI: 10.1021/ja804427q • Publication Date (Web): 11 October 2008

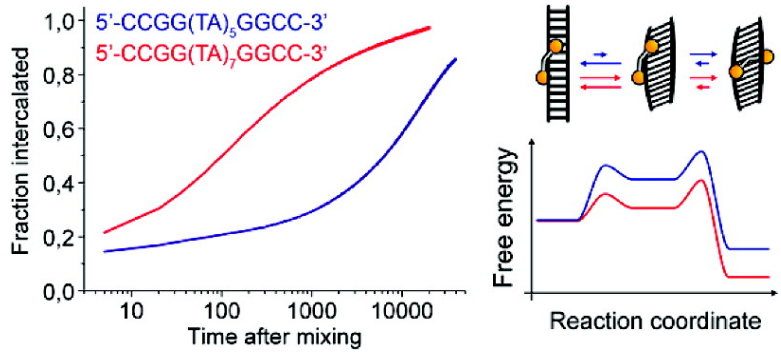

More About This Article

Additional resources and features associated with this article are available within the HTML version:

- Supporting Information
- Access to high resolution figures
- Links to articles and content related to this article
- Copyright permission to reproduce figures and/or text from this article

View the Full Text HTML

J|A|C|S
ARTICLES

Published on Web 10/11/2008

DNA Polymorphism as an Origin of Adenine-Thymine Tract Length-Dependent Threading Intercalation Rate

Pär Nordell,*,† Fredrik Westerlund,‡ Anna Reymer,† Afaf H. El-Sagheer,§,|| Tom Brown,§ Bengt Nordén,† and Per Lincoln†

Department of Chemical and Biological Engineering, Chalmers University of Technology, SE-41296 Gothenburg, Sweden, Nano-Science Center and Department of Chemistry, University of Copenhagen, DK-2100 Copenhagen, Denmark, School of Chemistry, University of Southampton, Highfield, Southampton SO17 1BJ, U.K., and Chemistry Department, Faculty of Petroleum and Mining Engineering, Suez Canal University, Suez, Egypt

Received June 11, 2008; E-mail: par.nordell@chalmers.se

Abstract: Binuclear ruthenium complexes that bind DNA by threading intercalation have recently been found to exhibit an exceptional kinetic selectivity for long polymeric adenine−thymine (AT) DNA. A series of oligonucleotide hairpin duplexes containing a central tract of 6−44 alternating AT base pairs have here been used to investigate the nature of the recognition mechanism. We find that, above a threshold AT tract length corresponding to one helix turn of B-DNA, a dramatic increase in threading intercalation rate occurs. In contrast, such length dependence is not observed for rates of unthreading. Intercalation by any mechanism that depends on the open end of the hairpin was found not to be important in the series of oligonucleotides used, as verified by including in the study a hairpin duplex cyclized by a copper-catalyzed "click" reaction. Our observations are interpreted in terms of a conformational pre-equilibrium, determined by the length of the AT tract. We finally find that mismatches or loops in the oligonucleotide facilitate the threading process, of interest for the development of mismatch-recognizing probes.

Introduction

DNA regions rich in adenine−thymine (AT) base pairs possess structural features that are essential for a number of biological processes. The selectivity of AT DNA stretches for small minor-groove binding drugs such as netropsin and pentamidine, as well as the selectivity for large TATA-box binding proteins, are well-known examples.[1−4] Whereas both involve direct recognition through a specific pattern of hydrogen bonds in the DNA grooves, the recognition mechanism in the second example also includes the ability of the duplex to adapt geometrically to the binding motif of the regulatory protein. Non-canonical DNA structures have been widely discussed in connection to poly-A tracts, which are rigid and associated with significant bending.[5−7] With alternating AT sequences, the duplex becomes more flexible.[8,9] The poor stacking and conformational freedom of the TpA step are factors that may account for an increased deformability.[10,11] It is no coincidence that AT-rich sequences frequently are found at functionally important locations such as promoter regions and origins of replication, in which control of unwinding, bending, and opening is essential for proper cell cycling.[5]

In this work we investigate the recently discovered exceptional kinetic selectivity for long, alternating AT stretches exhibited by a class of chiral binuclear ruthenium complexes, $[\mu\text{-(bidppz)}\mathbf{L}_4\text{Ru}_2]^{4+}$, with $\mathbf{L}$ = 2,2′-bipyridine (**B**) or 1,10-phenanthroline (**P**) and bidppz = 11,11′-bis-(dipyrido[3,2-*a*:2′,3′-*c*]phenazinyl) (Figure 1), which bind to DNA by threading intercalation. Passing one bulky coordinated Ru^{2+} center through the DNA double helix into or out of the intercalation site is an extremely slow process associated with a significant activation barrier.[12−14] Just like the mononuclear Ru complexes $[\text{Ru}\mathbf{L}_2\text{dppz}]^{2+}$,[15−18] intercalation of the extended dipyridophenazine ring system of the binuclear Ru complexes

† Chalmers University of Technology.
‡ University of Copenhagen.
§ University of Southampton.
|| Suez Canal University.

(1) Abu-Daya, A.; Brown, P. M.; Fox, K. R. *Nucleic Acids Res.* **1995**, *23*, 3385–3392.
(2) Wilson, D. W.; Nguyen, B.; Tanious, F. A.; Mathis, A.; Hall, J. E.; Stephens, C. E.; Boykin, D. W. *Curr. Med. Chem., Anti-Cancer Agents* **2005**, *5*, 389–408.
(3) Juo, Z. S.; Chiu, T. K.; Leiberman, P. M.; Baikalov, I.; Berk, A. J.; Dickerson, R. E. *J. Mol. Biol.* **1996**, *261*, 239–254.
(4) Davis, N. A.; Majee, S. S.; Kahn, J. D. *J. Mol. Biol.* **1999**, *291*, 249–265.
(5) Wang, J. C.; Cozzarelli, N. R. *DNA topology and its biological effects*; Cold Spring Harbor Laboratory Press: Cold Spring Harbor, NY, 1990.
(6) Barbic, A.; Zimmer, D. P.; Crothers, D. M. *Proc. Natl. Acad. Sci. U.S.A.* **2003**, *100*, 2369–2373.
(7) Rivetti, C.; Walker, C.; Bustamante, C. *J. Mol. Biol.* **1998**, *280*, 41–59.
(8) McClellan, J. A.; Palecek, E.; Lilley, D. M. J. *Nucleic Acids Res.* **1986**, *14*, 9291–9309.
(9) Yuan, H.; Quintana, J.; Dickerson, R. E. *Biochemistry* **1992**, *31*, 8009–8021.
(10) Klug, A.; Jack, A.; Viswamitra, M. A.; Kennard, O.; Shakked, Z.; Steitz, T. A. *J. Mol. Biol.* **1979**, *131*, 669–680.
(11) Suzuki, M.; Yagi, N.; Finch, J. T. *FEBS Lett.* **1996**, *379*, 148–152.
(12) Wilhelmsson, L. M.; Westerlund, F.; Lincoln, P.; Norden, B. *J. Am. Chem. Soc.* **2002**, *124*, 12092–12093.
(13) Nordell, P.; Westerlund, F.; Wilhelmsson, L. M.; Norden, B.; Lincoln, P. *Angew. Chem., Int. Ed.* **2007**, *46*, 2203–2206.
(14) Westerlund, F.; Nordell, P.; Norden, B.; Lincoln, P. *J. Phys. Chem. B* **2007**, *111*, 9132–9137.

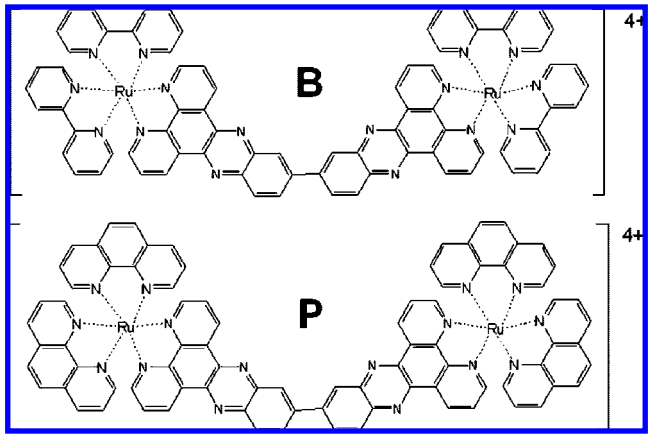

Figure 1. Structures of the semirigid binuclear ruthenium complexes in the current work, $[\mu\text{-(bidppz)}\mathbf{L}_4\mathrm{Ru}_2]^{4+}$, where $\mathbf{L} = 2,2'$-bipyridine (**B**, top) or 1,10-phenanthroline (**P**, bottom) and bidppz = 11,11′-bis(dipyrido[3,2-*a*:2′,3′-*c*]phenazinyl). The octahedral coordination of the Ru centers gives rise to two stereoisomeric forms: a right-handed (Δ) and a left-handed (Λ) propeller.

is accompanied by a very large increase in luminescence quantum yield (the "light-switch effect"),[12] allowing the process to be conveniently monitored by luminescence spectroscopy. Earlier kinetic studies with long polymeric DNA[12−14,19−21] have shown the rate of intercalation to depend sensitively on both size and stereochemistry of the Ru complex, and in particular on the DNA sequence composition: intercalation into poly-$(dAdT)_2$ is up to 3 orders of magnitude faster than that into mixed-sequence calf thymus DNA. The kinetic preference for long AT DNA has been suggested to be a result of collective duplex breathing dynamics as a rate-determining factor.[13]

For a series of oligonucleotide duplexes with a central alternating AT tract, the quantum yield of threaded ΔΔ-**P** increases gradually as the tract length is increased from 10 to 44 base pairs,[22] indicating that, at *equilibrium*, base pairs distant from the binding site exert a significant influence. Here we investigate the origin of the sequence-dependent *kinetic* discrimination of the threading intercalation process. A dramatically increased rate is observed when the AT tract length is extended from 10 to 14 base pairs, after which further lengthening only modestly increases the threading rate. However, the rate of dissociation is only slightly affected over this critical length interval. By studying a cyclized duplex, we verify that hairpin end effects are not important. Finally, we find that distorting features in the DNA duplex structure, such as mismatches or loops, can greatly facilitate the passage of the bulky Ru complex between the two strands, a property that could be of interest in the context of mismatch recognition probes.

Experimental Section

Materials. All experiments were conducted in 150 mM NaCl aqueous buffer (1 mM cacodylate, pH 7.0) unless otherwise stated.

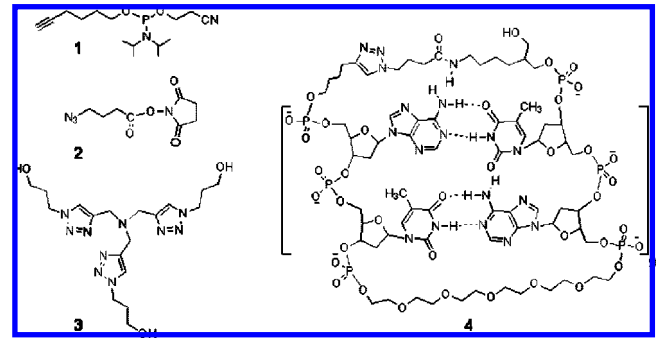

Figure 2. Functionalized hairpin oligonucleotide, chemical structures: hexynol phosphoramidite monomer (**1**); azidobutyrate active ester (**2**) and Cu(I) binding ligand (**3**); and cyclic nucleotide duplex (**4**) with hexaethylene glycol and 1,2,3-triazole linker.

Highly polymerized type I sodium salt calf thymus DNA, obtained from Sigma, was dissolved in buffer and filtered through a 0.8 μm Millipore filter before use. The sodium salt of polynucleotide poly$(dAdT)_2$, obtained from Amersham Biosciences, was dissolved in buffer and used without further purification. The concentration of DNA was estimated using extinction coefficients $\varepsilon_{260\mathrm{nm}} = 6600$ $\mathrm{M}^{-1}\ \mathrm{cm}^{-1}$ for calf thymus DNA, $\varepsilon_{262\mathrm{nm}} = 6600\ \mathrm{M}^{-1}\ \mathrm{cm}^{-1}$ for poly$(dAdT)_2$, and $\varepsilon_{254\mathrm{nm}} = 8400\ \mathrm{M}^{-1}\ \mathrm{cm}^{-1}$ for poly$(dGdC)_2$. Hexaethylene glycol (HEG)-linked hairpin oligonucleotides were obtained from ATDBio Ltd. (UK), dissolved in buffer, and reannealed (90 to 5 °C, 0.25 °C/min) before use. Extinction coefficients were calculated using OligoAnalyzer software, available online at www.idtdna.com. Ru complexes **B** and **P** were synthesized as described elsewhere,[12,16] and concentrations were estimated spectrophotometrically using extinction coefficients $\varepsilon_{412\mathrm{nm}} = 65\,000$ and 75 800 $\mathrm{M}^{-1}\ \mathrm{cm}^{-1}$, respectively.

Synthesis. a. 5′-Alkyne- and 3′-Azide-Functionalized Hairpin Oligonucleotide. The hairpin oligonucleotide 5′-alkyne-$(AT)_9$-HEG-$(AT)_9$-amino-3′ was synthesized on an ABI-394 DNA synthesizer using a standard "trityl-on" 1.0 μmol phosphoramidite cycle of deprotection, coupling, capping, and oxidation, using a 1.0 μmol aminolink C7 synthesis column (Link Technologies) to incorporate the 3′-amine. The 5′-alkyne phosphoramidite (**1** in Figure 2) and HEG monomer (spacer-18, Link Technologies) were coupled for 8 min, and all other monomers were coupled for 40 s. The oligonucleotide was then cleaved from the solid support by treatment with concentrated aqueous ammonia for 1 h at room temperature and deprotected by heating at 55 °C for 5 h in the same reagent. The crude oligonucleotide was gel-filtered on a disposable NAP-10 column (GE Healthcare) and freeze-dried before labeling the 3′-amino group with 4-azidobutyrate *N*-hydroxysuccinimide (NHS) ester (**2** in Figure 2). The azide NHS ester (2 mg) was dissolved in dimethylsulfoxide (40 μL) and added to the oligonucleotide, which was dissolved in 80 μL of 0.5 M Na_2CO_3/$NaHCO_3$ buffer, pH 8.75. The mixture was left to react at room temperature for 4 h.[23] The fully labeled oligonucleotide was gel-filtered as described above and then purified by reversed-phase high-performance liquid chromatography (HPLC) (octyl, C8) in a gradient of acetonitrile in 0.1 M ammonium acetate and desalted by gel filtration using a disposable NAP-10 column (GE Healthcare).[24]

b. Oligonucleotide Cyclization. Sodium ascorbate (10.0 μmol in 20.0 μL of 200 mM NaCl) was added to a solution of tris-hydroxypropyl triazole ligand[25] (**3** in Figure 2) (7.0 μmol in

(15) Friedman, A. E.; Chambron, J. C.; Sauvage, J. P.; Turro, N. J.; Barton, J. K. *J. Am. Chem. Soc.* **1990**, *112*, 4960–4962.
(16) Hiort, C.; Lincoln, P.; Norden, B. *J. Am. Chem. Soc.* **1993**, *115*, 3448–3454.
(17) Haq, I.; Lincoln, P.; Suh, D. C.; Norden, B.; Chowdhry, B. Z.; Chaires, J. B. *J. Am. Chem. Soc.* **1995**, *117*, 4788–4796.
(18) Holmlin, R. E.; Stemp, E. D. A.; Barton, J. K. *Inorg. Chem.* **1998**, *37*, 29–34.
(19) Lincoln, P.; Norden, B. *Chem. Commun.* **1996**, 2145–2146.
(20) Nordell, P.; Lincoln, P. *J. Am. Chem. Soc.* **2005**, *127*, 9670–9671.
(21) Westerlund, F.; Nordell, P.; Blechinger, J.; Santos, T. M.; Nordén, B.; Lincoln, P. *J. Phys. Chem. B* **2008**, *112*, 6688–6694.
(22) Westerlund, F.; Lincoln, P. *Biophys. Chem.* **2007**, *129*, 11–17.
(23) Kumar, R.; El-Sagheer, A.; Tumpane, J.; Lincoln, P.; Wilhelmsson, L. M.; Brown, T. *J. Am. Chem. Soc.* **2007**, *129*, 6859–6864.
(24) El-Sagheer, A. H.; Kumar, R.; Findlow, S.; Werner, J. M.; Lane, A. N.; Brown, T. *ChemBiochem* **2008**, *9*, 50–52.
(25) Chan, T. R.; Hilgraf, R.; Sharpless, K. B.; Fokin, V. V. *Org. Lett.* **2004**, *6*, 2853–2855.

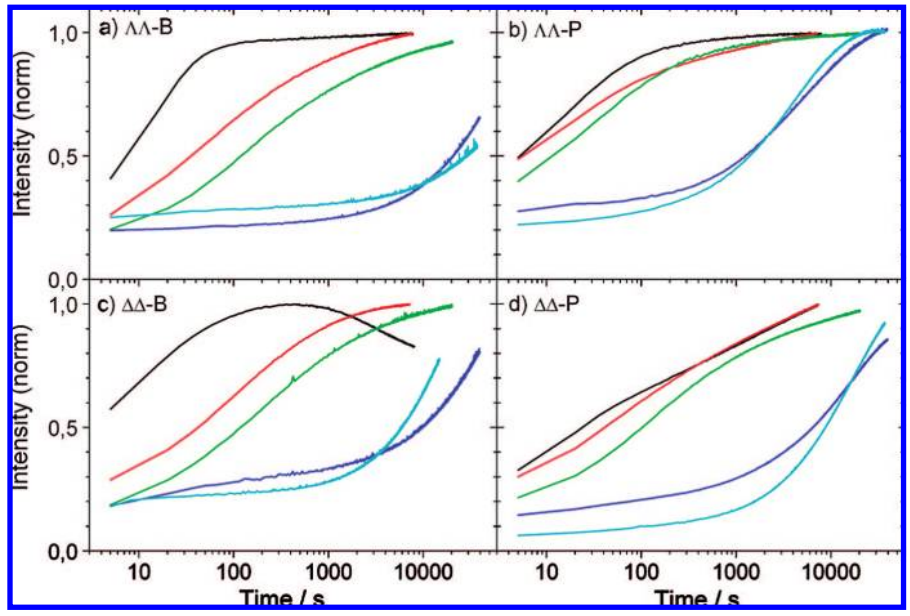

Figure 3. Sequence dependence: luminescence after mixing (a) ΛΛ-**B**, (b) ΛΛ-**P**, (c) ΔΔ-**B**, or (d) ΔΔ-**P** with DNA at 37 °C, normalized to final/maximum intensity. Color coding: poly(dAdT)$_2$, black; **X** = (TA)$_{11}$, red; **X** = (TA)$_7$, green; **X** = (TA)$_5$, blue; and calf thymus DNA, cyan.

1.65 mL in 200 mM NaCl) under argon. This was followed by the addition of $CuSO_4 \cdot 5H_2O$ (1.0 μmol in 10 μL of 200 mM NaCl). The 5′-alkyne- and 3′-azide-functionalized hairpin oligonucleotide (20.0 nmol in 0.82 mL of 200 mM NaCl) was heated at 80 °C for 5 min, cooled slowly, and added to the above solution. The reaction mixture was kept under argon at room temperature for 2 h, and a disposable NAP-25 gel-filtration column was used to remove reagents (GE Healthcare). The conversion was almost quantitative, as shown by HPLC (Figure S4, Supporting Information) and capillary electrophoresis (CE) (Figure S5, Supporting Information). The cyclic oligonucleotide (**4** in Figure 2) was purified by reversed-phase HPLC using a C8 column and a gradient of acetonitrile in 0.1 M ammonium acetate,[24] followed by NAP-10 gel filtration to give 52% isolated yield. Results from mass spectra analysis are given in Table S3 (Supporting Information).

Methods. The concentrations used in the time-dependent experiments were, unless otherwise stated, [Ru complex] = 1 μM and [HEG-linked duplex] = 1 μM, and for the polynucleotides, calf thymus DNA [nucleobase] = 36 μM and poly(dAdT)$_2$ and poly(dGdC)$_2$ [nucleobase] = 50 μM. Luminescence experiments were performed on a Varian Cary Eclipse spectrofluorimeter. Samples were excited at 410 nm, and emission was recorded at 650 nm. After the major part of the association process had been followed spectroscopically, samples were incubated at the same temperature for 2−4 days, after which the final intensity was recorded. For the dissociation experiments, a stock solution of 3.0% w/w sodium dodecyl sulfate (SDS) in buffer was mixed with samples of DNA and Ru complex to obtain a final detergent concentration of 0.6% w/w. When poly(dAdT)$_2$ was used as an alternative scavenger of dissociated Ru complex, polynucleotide was added to pre-equilibrated samples from a stock solution to attain a final [poly(dAdT)$_2$] = 50 μM. Circular dichroism (CD) spectra were measured on a Jasco J-810 spectropolarimeter between 550 and 220 nm using a 5 mm quartz cell. Differential spectra, CD(t=0) − CD(t), were collected as columns into a matrix **M**. By using the MatLab computational software, **M** was factorized into three matrices (SVD, singular value decomposition):

$$\mathbf{M} = \mathbf{U} \times \mathbf{S} \times \mathbf{V}^{\mathrm{T}} \qquad (1)$$

where **U** and **V** have orthonormal columns and the elements of **S** are zero except for the diagonal, which are the non-negative singular values $s_1 \geq s_2 \geq \ldots \geq 0$. The SVD analysis of the difference spectra in **M** is a model-free evaluation of the number of different DNA-binding modes that can be detected by CD. The number of singular values that are significantly larger than the rest gives the number of linearly independent species, i.e., physical species with distinctly different spectra, in the data set **M**. If only one significant species is present, the first column of **U** multiplied by s_1 corresponds to its spectrum, and the first column of **V** corresponds to the time evolution of its concentration, the remaining columns of **U** and **V** containing the noise of the data set.

Model structures were assembled by manual docking of ΔΔ-**P** in (AT)$_7$ oligonucleotide duplexes of B- and A-form. Docking was followed by geometry optimization in the Amber force field with the HyperChem 7.52 program package.

Results

A series of HEG-linked hairpin oligonucleotides (5′-CCG-G**X**GGCC-HEG-GGCC**X**CCGG-3′, **X** = (TA)$_3$ to (TA)$_{22}$, where TA indicates a T-A base pair followed by an A-T base pair) containing a central tract of 6−44 AT base pairs were used to investigate the dependence of the threading intercalation rate on AT tract length for four binuclear ruthenium complexes: **B** and **P** in ΔΔ and ΛΛ conformations (Figure 1). The thermal stability of the HEG-linked hairpin duplexes was found to be virtually independent of AT tract length, with T_m values in the range 65−66 °C (Figure S3, Supporting Information). The kinetic studies were carried out at 25, 37, or 50 °C to probe the wide range of rates observed with different oligonucleotide sequences.

AT Tract Recognition. The collection of kinetic traces in Figure 3 shows how the normalized luminescence intensity increases after mixing each of the four Ru complexes with calf thymus DNA, poly(dAdT)$_2$, or AT-containing hairpins with terminal GC regions, where **X** = (TA)$_5$, (TA)$_7$, or (TA)$_{11}$, at 37 °C (1:1 duplex:Ru complex ratio). With the shorter hairpin **X** = (TA)$_3$, the emission intensity remains low and virtually unaltered after mixing (not shown), indicating that the rearrangement to the threaded state in hairpins with AT tract lengths up to 6 base pairs is very unfavorable. For all Ru complexes, the traces for **X** = (TA)$_5$ and calf thymus DNA are very similar, with half-completion times ($t_{1/2}$) ranging between 20 min (ΛΛ-**P**) and 5 h (ΛΛ-**B**) (Table S1, Supporting Information). The

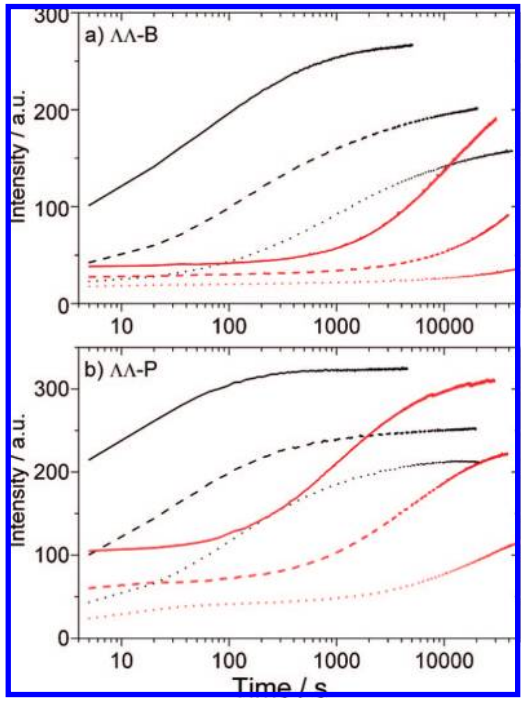

Figure 4. Temperature dependence: luminescence intensity after mixing (a) ΛΛ-**B** or (b) ΛΛ-**P** with hairpin $\mathbf{X} = (TA)_7$ (black) or $\mathbf{X} = (TA)_5$ (red) at 50 (—), 37 (---), and 25 °C (•••).

kinetics are abruptly changed when the AT tract is lengthened by 4 base pairs: threading into $\mathbf{X} = (TA)_7$ is around 2 orders of magnitude faster than with $\mathbf{X} = (TA)_5$ for all four Ru complexes. However, further lengthening the tract by 8 AT base pairs to $\mathbf{X} = (TA)_{11}$ only increases the rates by approximately a factor of 3. Thus, an increase of the AT tract length from 1 to 1.4 helix turns appears to be critical for fast threading. Extension beyond $\mathbf{X} = (TA)_{11}$ gives, as expected, gradually increased rates, approaching that observed with poly(dAdT)$_2$. The increase is, however, moderate, and even with 4.4 helix turns of AT base pairs ($\mathbf{X} = (TA)_{22}$), all four Ru complexes still display kinetics clearly different from that with the long AT polymer (Figure S1, Supporting Information).

Temperature and Mixing-Ratio Dependence. The behavior of the hairpin duplexes is similar to that of mixed-sequence DNA,[13] with ΛΛ-**P** generally attaining its final luminescence intensity considerably faster than its analogues. ΛΛ-**B** exhibits the slowest threading, but at elevated temperature (50 °C) most of the process, even with $\mathbf{X} = (TA)_5$, is completed within a few hours. Together with traces obtained at 25 and 37 °C, several interesting qualitative aspects of binding for the two ΛΛ enantiomers are apparent (Figure 4). First, the threading kinetics changes completely upon extension of the AT tract from $\mathbf{X} = (TA)_5$ to $\mathbf{X} = (TA)_7$. Second, there is a strong temperature dependence for the threading rates into both hairpins. Third, for ΛΛ-**B** especially, only a small luminescence increase is detected during the course of the measurement for $\mathbf{X} = (TA)_5$ (~15 h) at 25 °C. Fourth, a significant difference is observed between the final luminescence intensities obtained at the three temperatures. The "rate leap" between the two AT tract lengths is only slightly dependent on the duplex:Ru complex mixing ratio (Figure S2, Supporting Information, shows traces at ratios between 1:2 and 2:1 with ΔΔ-**P**).

Kinetic Analysis. Luminescence kinetic data for Ru complexes binding to $\mathbf{X} = (TA)_7$ generally require at least two exponentials for a satisfactory fit. We have previously shown that, after threading is completed, a slow redistribution of threaded Ru complexes in the DNA lattice can alter the luminescence quantum yield, [21,26] which suggests that the fastest phase is most representative of the actual intercalation step. In general, this process is found to account for >70% of the total luminescence increase of analyzed traces fitted with a biexponential expression (not shown). The first inverse rate constant obtained with $\mathbf{X} = (TA)_7$ at 37 °C is 85 s for ΛΛ-**P** and in the range 250−280 s for the three other Ru complexes. An accurate determination of kinetic parameters for $\mathbf{X} = (TA)_5$ is difficult, even at 50 °C, but on the basis of $t_{1/2}$ of emission traces in Figure 2, the rates are estimated to be between 180 (ΛΛ-**B**) and 65 (ΔΔ-**P**) times slower than with $\mathbf{X} = (TA)_7$ (Table S1, Supporting Information).

By studying the evolution of the CD spectral shape after mixing, the actual threading step can be separated from subsequent processes included in the binding.[21] Using CD, we have earlier shown that, despite the apparent complexity of the luminescence data, the initial threading into poly(dAdT)$_2$ of all four Ru complexes does, in fact, follow a simple first-order rate law. Binding of ΛΛ-**B** to the short $\mathbf{X} = (TA)_3$ and long $\mathbf{X} = (TA)_{22}$ hairpins was studied by CD and compared to binding to poly(dAdT)$_2$. At 25 °C, a gradual change of the CD spectrum with $\mathbf{X} = (TA)_{22}$ is observed throughout the binding process, similar to that observed with the AT polymer. With $\mathbf{X} = (TA)_3$, on the other hand, no spectral changes with time are detected, even when the temperature is increased to 50 °C for several hours. Differential spectral data were analyzed by SVD (see Experimental Section), from which one main component, well-defined in both the spectral (u_1) and time (v_1) domains, was obtained for $\mathbf{X} = (TA)_{22}$. Figure 5 presents the results together with corresponding data for poly(dAdT)$_2$. Even though the amplitudes differ, the spectral shapes of u_1 overlap very well, suggesting that the rearrangement from an externally bound state to the intercalated geometry is very similar in the two types of DNA. By contrast, while v_1 for poly(dAdT)$_2$ fits well to a first-order rate expression, v_1 for the $\mathbf{X} = (TA)_{22}$ hairpin is clearly multiphasic. Analysis of the $\mathbf{X} = (TA)_3$ CD data produces only unstructured components with low amplitude, as would be expected when the threading is inefficient.

Dissociation. Sequestering by SDS, which both shifts the equilibrium and catalyzes the unthreading process,[14,27] provides a simple tool to differentiate between the rapid dissociation of groove binding and the very slow dissociation from the threaded state. Addition of SDS to a sample of Ru complex and mixed-sequence DNA within a few minutes after mixing results in a practically instantaneous drop in emission intensity to that observed for the Ru complex bound to SDS micelles alone. However, for an equilibrated sample, the change in emission after addition of SDS is very slow.[12] Threading is faster into poly(dAdT)$_2$, and a considerable fraction of the Ru complexes dissociate slowly, even when SDS is added directly after mixing.

A series of SDS sequestering experiments were performed with ΔΔ-**P** to verify that the luminescence intensity increase indeed is representative of the amount of threaded Ru complex also for the oligonucleotide hairpins. Five minutes after mixing ΔΔ-**P** with hairpin $\mathbf{X} = (TA)_7$ at 37 °C, only about 20% of the Ru complex dissociates within a few seconds, as determined from SDS sequestering (Figure 6a). This indicates that a large

(26) Westerlund, F.; Wilhelmsson, L. M.; Norden, B.; Lincoln, P. *J. Phys. Chem. B* **2005**, *109*, 21140–21144.
(27) Westerlund, F.; Wilhelmsson, L. M.; Norden, B.; Lincoln, P. *J. Am. Chem. Soc.* **2003**, *125*, 3773–3779.

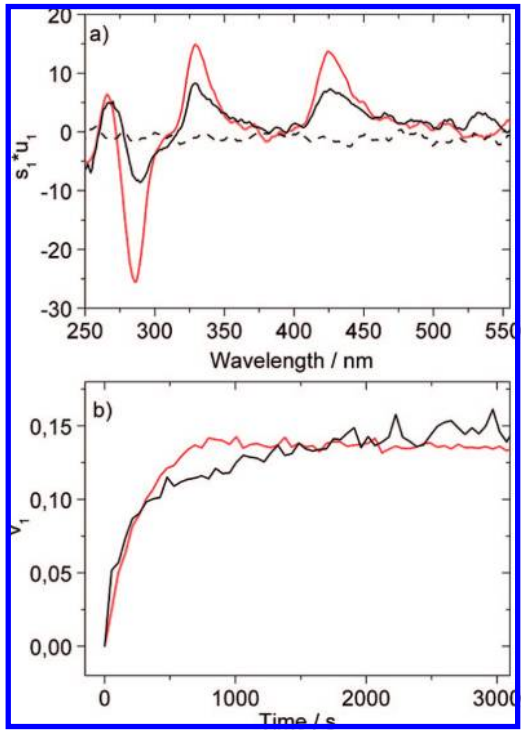

Figure 5. Time evolution of the CD spectrum: ΛΛ-**B** binding to hairpin **X** = $(TA)_{22}$ (black) or poly(dAdT)2 (red) at 25 °C. (a) Main spectral component u_1 multiplied by its weight s_1. With hairpin **X** = $(TA)_3$ (---), no structured spectral component was obtained, even after the temperature was raised to 50 °C for several hours. (b) Time evolution v_1 of the main spectral component. [Ru complex] = 2 μM, [HEG-linked duplex] = 2 μM, and poly$(dAdT)_2$ [nucleobase] = 72 μM.

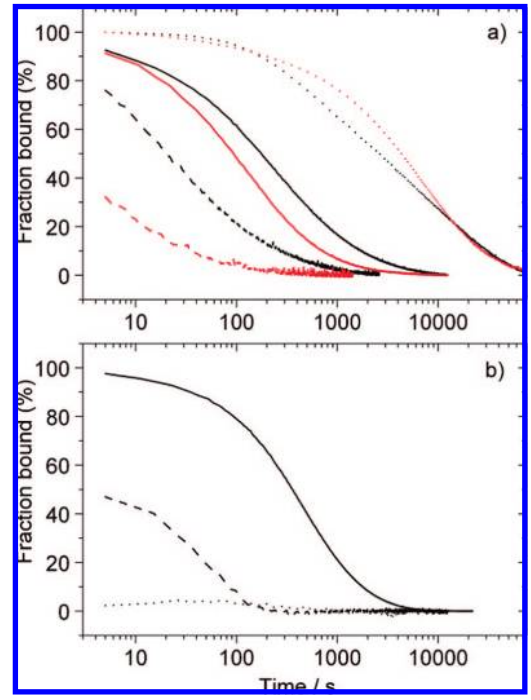

Figure 6. Dissociation: fraction of bound Ru complex after addition of SDS at 37 °C or poly$(dAdT)_2$ at 50 °C to samples of ΔΔ-**P** mixed with DNA. Intensity prior to addition and in SDS micelles/poly$(dAdT)_2$ normalized to 100 and 0%, respectively (data corrected for dilution). (a) Addition of SDS 5 min (---), SDS 24 h (—), or poly$(dAdT)_2$ 24 h (•••) after mixing ΔΔ-**P** with hairpin **X** = $(TA)_7$ (black) or $(TA)_5$ (red). (b) SDS addition to samples of ΔΔ-**P** with poly$(dAdT)_2$ 5 min after mixing (—) and with poly$(dGdC)_2$ (---) or hairpin **X** = $(AT)_2GC(AT)_2$ (•••) 24 h after mixing.

fraction of the Ru complex is threaded already at this stage of the binding process. With the shorter **X** = $(TA)_5$, roughly 65% dissociates directly, consistent with the slower binding kinetics observed from the luminescence intensity increase. For samples that have been incubated for 24 h at 37 °C, more than 90% of the Ru complexes are dissociating slowly from both hairpins, showing that, even if the kinetics differ, almost all complexes can eventually thread also into the shorter **X** = $(TA)_5$ tract, given sufficient time. Further shortening to **X** = $(TA)_3$, for which the emission intensity remains comparably low and unaltered, even at 50 °C, gives instant release of virtually all Ru complexes also after very long equilibration times (>24 h, data not shown).

The SDS sequestering traces with the hairpins can be compared to those obtained with AT and GC polymers. The bottom panel of Figure 6 shows dissociation upon SDS addition to samples in which ΔΔ-**P** has been incubated with poly$(dAdT)_2$ for five minutes or with poly$(dGdC)_2$ for 24 h at 37 °C. No immediate dissociation is observed after detergent addition to the sample with the AT polymer, while 50% is quickly dissociated from GC-DNA, despite the much longer equilibration time. The remaining fraction is released within 2 min, in sharp contrast to the very slow dissociation from the AT polymer. The rapid SDS sequestration and the very low quantum yield suggest that the Ru complexes are not threaded−intercalated in GC-DNA. Interestingly, when the two middle AT base pairs in **X** = $(TA)_5$ are replaced by two GC base pairs (**X** = $(TA)_2GC(TA)_2$), the luminescence quantum yield is dramatically decreased, and virtually all Ru complexes are dissociated instantly—even after long incubation times (Figure 6b)—again showing how GC base pairs effectively prevent threading.

We have also used poly$(dAdT)_2$ as a sequestering agent, a method recently developed to avoid the catalytic effect of SDS and other detergents on the dissociation.[14] Addition of poly$(dAdT)_2$ to a pre-equilibrated sample of Ru complex and mixed-sequence DNA results in a redistribution to the thermodynamically favored AT DNA binding sites, without any significant perturbation of the true dissociation kinetics. Consequently, the luminescence spectrum gradually shifts to that expected for a sample containing only Ru complex bound to poly$(dAdT)_2$. As binding to poly$(dAdT)_2$ is comparably fast, the spectral evolution reflects the intrinsic unthreading rate of Ru complexes from intercalation sites in mixed-sequence DNA. The same approach proved to be applicable for probing dissociation from the hairpins. In contrast to the almost 2 orders of magnitude difference in association rates, dissociation rates of ΔΔ-**P** from **X** = $(TA)_5$ and $(TA)_7$, as determined by poly$(dAdT)_2$ sequestering at 50 °C, are very similar, and 90% dissociation occurs within 8 h (Figure 6a). While this is very slow, it is significantly faster than dissociation from mixed-sequence DNA, for which the corresponding time exceeds 30 h.[14]

Hairpin End Effects. To investigate to what extent the difference in behavior between poly$(dAdT)_2$ and long AT tract hairpins can be attributed to the terminal CCGG sequences, hairpins consisting exclusively of alternating AT base pairs ($(TA)_n^0$, where ^{0} indicates no end GC base pairs, see Table 1) were studied. Surprisingly, threading intercalation of ΔΔ-**P** into $(TA)_7^0$ without GC ends is considerably faster than that into the much longer **X** = $(TA)_{22}$ hairpin flanked by GC (Figure 7a). In fact, binding proceeds at an overall rate comparable to that with poly$(dAdT)_2$, even though the kinetics remains clearly

Table 1. Sequences of Oligonucleotide Hairpins

code	hairpin sequence
X = $(TA)_n$, $n = 3-22$	5′-CCGG(**TA**)$_n$GGCC-HEG-GGCC(**TA**)$_n$CCGG-3′
$(TA)_7{}^0$	5′-(**TA**)$_7$-HEG-(**TA**)$_7$-3′
$(AT)_9{}^a$	5′-(**AT**)$_9$-HEG-(**AT**)$_9$-3′
$(TA)_7{}^{cc}$	5′-CCGG(**TA**)$_3$**CA**(**TA**)$_3$GGCC-HEG-GGCC(**TA**)$_3$**TC**(**TA**)$_3$CCGG-3′
$(TA)_{8:7}$	5′-CCGG(**TA**)$_8$GGCC-HEG-GGCC(**TA**)$_7$CCGG-3′
$(TA)_{14:7}$	5′-CCGG(**TA**)$_{14}$GGCC-HEG-GGCC(**TA**)$_7$CCGG-3′

[a] In open hairpin and cyclic forms (see Experimental Section). HEG = hexaethylene glycol.

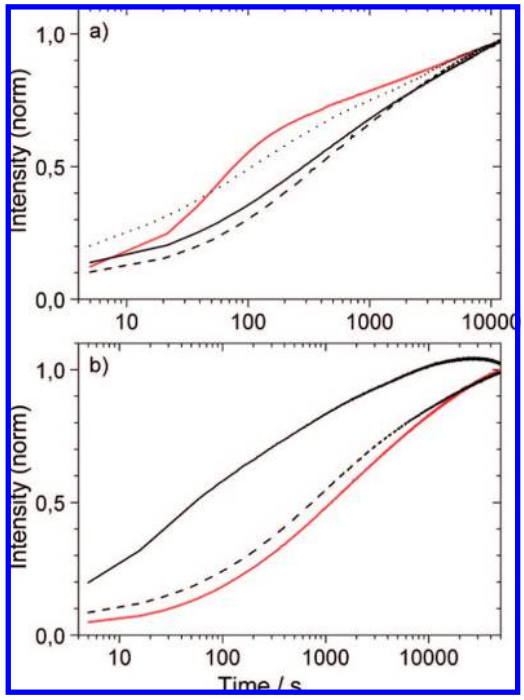

Figure 7. Hairpin end effects: luminescence intensity after mixing ΔΔ-**P** and DNA at 25 °C. (a) Hairpin with CCGG ends (**X** = $(TA)_{22}$ (—) and $(TA)_7$ (---)), compared to hairpin without ($(TA)_7{}^0$ (•••)). Trace with poly(dAdT)$_2$ in red. Data normalized at 10 000 s. (b) Open (—) and closed (---) $(AT)_9{}^0$ hairpins. CCGG end reference **X** = $(TA)_9$ in red. Data normalized at 50 000 s. Note the different *x*-axis scales.

different. The flanking CCGG base pairs thus have a considerable effect on the binding rate.

Studies of a 5′-alkyne- and 3′-azide-functionalized AT hairpin oligonucleotide $(AT)_9{}^0$ (Table 1), which can be covalently cyclized by a copper-catalyzed "click" reaction[23] (see Experimental Section), give further insight into the mechanisms behind this finding (Figure 7b). With the "open" hairpin form, binding of ΔΔ-**P** resembles that to the shorter $(TA)_7{}^0$. Cyclization of the $(AT)_9{}^0$ hairpin prevents the end from fraying and has a stabilizing effect on the duplex,[24] as demonstrated by the increased melting temperature of the cyclic relative to the open hairpin duplex (Figure S6, Supporting Information). Quite remarkably, with the cyclized duplex, the kinetics resembles the considerably slower binding to the corresponding hairpin with CCGG ends (**X** = $(TA)_9$). The results indicate that the presence of four flanking GC base pairs, as effectively as a covalent closure, prevents Ru complexes from entering by any mechanism that depends upon fraying at the end of the hairpin.

Mismatch Recognition. Incorrect insertions, deletions, or incorporations of bases during DNA replication and recombination are potential threats to the genetic stability of a cell.

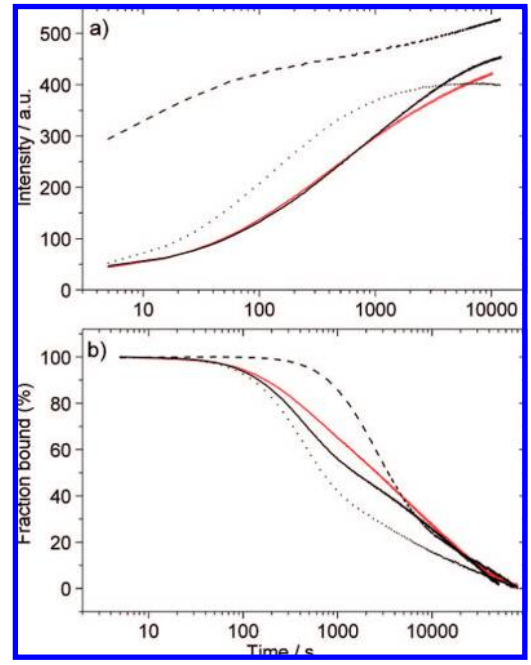

Figure 8. Interaction with imperfect DNA. (a) Luminescence after mixing ΔΔ-**P** and hairpin at 25 °C. (b) Addition of poly(dAdT)$_2$ at 50 °C to samples of ΔΔ-**P** pre-equilibrated with hairpin for 24 h. Coding: $(TA)_{8:7}$ (—), $(TA)_{14:7}$ (---), and $(TA)_7{}^{cc}$ (•••), and **X** = $(TA)_7$ (red). Sequences of the hairpins are given in Table 1. Note the different *x*-axis scales.

Understanding how small molecules can recognize such noncomplementary regions in DNA could lead to the development of new biophysical or diagnostic tools.[28] As mutational elements often are accompanied by local distortions of the duplex structure,[29] passage of bulky structures between the strands might be facilitated. Experiments were performed to investigate whether such alternative structures could act as "entrance doors" for threading of Ru complexes. Using the **X** = $(TA)_7$ hairpin as a Watson−Crick base-pairing reference, three different modifications were introduced to create a small bulge ($(TA)_{8:7}$), a loop ($(TA)_{14:7}$), or a CC mismatch ($(TA)_7{}^{cc}$) (see Table 1 for sequences). Figure 8a shows luminescence traces after mixing ΔΔ-**P** with the three hairpins at 25 °C, together with the trace obtained for **X** = $(TA)_7$. Addition of two extra bases to one strand ($(TA)_{8:7}$) has practically no effect on the binding kinetics, as indicated by the almost identical luminescence traces. A larger hairpin loop ($(TA)_{14:7}$), on the other hand, has a dramatic effect. More than half of the intensity normally observed 3 h after mixing is reached within a few seconds, indicative of a very large fraction being instantly intercalated. This effect is not just a consequence of an increased number of AT base pairs, because binding to AT tracts much longer than 14 base pairs displays kinetics not very different from that with **X** = $(TA)_7$ (Figure 8a). Insertion of an unstable mismatch also markedly facilitates threading: the rate for the CC mismatched hairpin, $(TA)_7{}^{cc}$, is almost 4 times as high as for the fully base-paired sequence.

To study dissociation from the imperfectly paired DNA, samples of ΔΔ-**P** and hairpins were equilibrated for 24 h at 50 °C and then mixed with poly(dAdT)$_2$ to sequester the Ru complexes at the same temperature (Figure 8b). The highest

(28) Bui, C. T.; Rees, K.; Lambrinakos, A.; Bedir, A.; Cotton, R. G. H. *Bioorg. Chem.* **2002**, *30*, 216–232.
(29) Moe, J. G.; Russu, I. M. *Biochemistry* **1992**, *31*, 8421–8428.

dissociation rate is observed for $(TA)_7^{cc}$, followed by $(TA)_{8:7}$ and $\mathbf{X} = (TA)_7$, while the dissociation from $(TA)_{14:7}$ is the slowest. Hence, a small bulge has only a modest effect on association and dissociation, a CC mismatch facilitates both processes, and a larger loop increases the threading rate dramatically and stabilizes the intercalated state. Approximate $t_{1/2}$ values of association and dissociation are given in Table S2 (Supporting Information).

Discussion

The results presented here identify the extension from 10 to 14 base pairs as a critical interval of AT tract length, over which the binding rates by threading intercalation for all four studied binuclear ruthenium complexes increase dramatically. The observation that the DNA sequence distant from the intercalation site influences the kinetics and affinity is important and raises the question of the nature of the communication mechanism. Due to its cooperativity, duplex melting might be considered a plausible cause. However, the hairpin duplex melting temperature ($T_m = 65-66$ °C) is found to be virtually invariant with the AT tract length and very similar to the value for poly(dAdT)$_2$ under the same conditions ($T_m = 63$ °C). The structural polymorphism of DNA could offer an alternative explanation for long-range sequence-dependent properties. The deformability of particular DNA sequences has been suggested to be a basis for the recognition of, e.g., the TATA-box binding proteins.[3] Furthermore, long, alternating AT tracts have been shown to be especially susceptible to chemical and enzymatic modifications, indicating that, above a certain length, this type of DNA is especially prone to adopt alternative conformations.[8] In fact, structural changes resulting from binding of ligands to alternating AT base pairs at a distance from the principal site of interaction were earlier observed for actinomycin D.[30] The Ru complexes studied here are large, rigid, and highly charged molecules that are likely to influence the conformation of the DNA polyanion.

In sharp contrast to the forward threading rate, the rate of unthreading is only slightly affected by the AT tract lengthening from 10 to 14 base pairs. The diverse dependence of the association and dissociation events on tract length can be interpreted in terms of a simple pre-equilibrium model (Figure 9). Ru complexes initially associate externally with the hairpins in their native form. A local conformational distortion can be induced around the binding site, for which the free energy increase will depend on the size of the AT tract: the junction tension between the locally deformed DNA and the surrounding unperturbed ends will be reduced when distributed over a longer stretch of easier-deformable AT base pairs. The subsequent threading step may not require the opening of more than one base pair,[31] making the associated energy barrier highly sensitive to the structure of the Ru center which has to pass,[13,14,20,21] but insensitive to the length of the whole AT tract. While the rate of formation of a threaded state is limited by both the pre-equilibrium between two DNA conformations and the actual threading between the DNA strands, the rate-limiting step of dissociation is unthreading only. Assuming the pre-equilibrium, but not the threading step, to depend on the AT tract length increase from 10 to 14 base pairs, this model will lead to similar

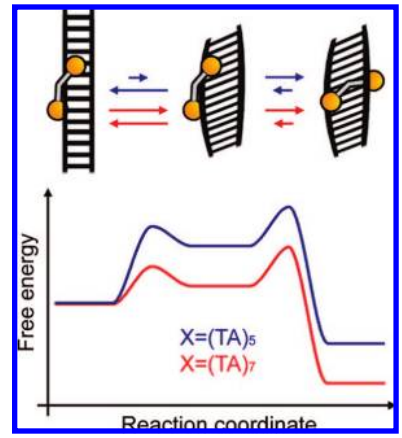

Figure 9. (Top) Illustration of proposed model of binding. See text for details. (Bottom) Schematic energy diagram for duplex hairpins $\mathbf{X} = (TA)_5$ (blue) and $(TA)_7$ (red).

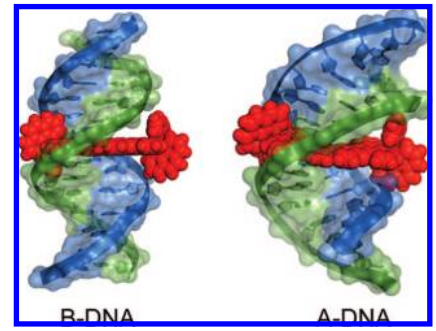

Figure 10. Two models of the final intercalated binding geometry of ΔΔ-**P** in a $(AT)_7$ oligonucleotide duplex, with one Ru(phen)$_2$ moiety positioned deeply in the minor groove. Compared to B-form DNA (left), DNA in A-form DNA (right) allows more favorable accommodation of the Ru complex; it provides increased electrostatic attraction in the major groove. Illustrations were prepared with Pymol (http://pymol.sourceforge.net/).

dissociation but different association rates. If the free energy of the initial association of the Ru complex with the native DNA is used as a reference, the free energy of the threaded state will be lower for the $\mathbf{X} = (TA)_7$ compared to the $\mathbf{X} = (TA)_5$ sequences (Figure 9). This is not unreasonable, considering the thermodynamic preference for the infinite AT tract binding sites in poly(dAdT)$_2$ displayed in the dissociation studies.

Additional experiments with modified hairpins and ΔΔ-**P** were performed to further investigate the sequence dependence and hairpin end effects, as well as to study the influence of base-pairing imperfections. Several interesting aspects of the interaction were observed. First, the cyclized AT tract hairpin duplex $(AT)_9^0$ gives rise to a threading kinetics that closely resembles that for the corresponding AT tract with terminal CCGG sequences, $\mathbf{X} = (TA)_9$. However, with the uncyclized $(AT)_9^0$ as well as with $(TA)_7^0$ hairpins, significantly higher intercalation rates are observed (Figure 7). The results show that, for AT tracts sealed by GC regions, like in polymeric DNA, the intercalated state is formed by threading between the strands (internal threading) rather than by a mechanism that depends on the open end of the hairpin. By contrast, with AT as terminal base pairs, the end will have a higher tendency to fray, which could offer Ru complexes a low energy barrier route to intercalation.

Fast, "AT DNA-like", internal threading of ΔΔ-**P** is thus seen with the cyclized $(AT)_9^0$ hairpin. Replacement of AT base pairs by GC in the 18-mer duplex dramatically decreases the

(30) Lane, M. J.; Laplante, S.; Rehfuss, R. P.; Borer, P. N.; Cantor, C. R. *Nucleic Acids Res.* **1987**, *15*, 839–852.
(31) Paramanathan, T.; Westerlund, F.; McCauley, M. J.; Rouzina, I.; Lincoln, P.; Williams, M. C. *J. Am. Chem. Soc.* **2008**, *130*, 3752–3753.

intercalation rate: substitution of the eight flanking AT base pairs with GC in the open $(AT)_9{}^0$ hairpin gives $\mathbf{X} = (TA)_5$, which in terms of threading kinetics can be considered as "ct-DNA-like". A further substitution of the two central AT base pairs by GC gives $\mathbf{X} = (AT)_2GC(AT)_2$, for which no signs of threading intercalation are observed: absence of the "light-switch" effect, no change in CD, and practically instantaneous sequestration of the Ru complex by SDS micelles. Thus, for an 18-base-pair-long duplex, internal threading ranges from very inefficient with $\mathbf{X} = (TA)_2GC(TA)_2$, via slow with $\mathbf{X} = (TA)_5$ ($t_{1/2} \sim$ hours at 37 °C), to fast with cyclized $(AT)_9{}^0$ ($t_{1/2} \sim$ minutes at 37 °C).

Finally, we find that different types of base-pairing imperfections have various effects on association and dissociation rates. A small bulge has virtually no effect on binding by threading and only doubles the rate of unthreading, suggesting that small migrating "bubbles" in repeat sequences are not major rate-determining events. A static opening within the duplex formed by the unstable CC mismatch has a larger effect. The rates of both threading and unthreading are increased by a factor of 4. Introduction of a large AT-loop has, however, the most dramatic effect. Threading becomes very rapid, while the dissociation is slowed considerably. Compared to the small bulge, one could expect that the more flexible nature of the unpaired junction between the loop and the duplex would allow both faster threading and tighter binding of a Ru complex. Even though the multiphasic nature of the kinetic data makes quantitative comparison of thermodynamic parameters difficult, the affinity of ΔΔ-**P** can be scored on the basis of the half-times, $t_{1/2}$, of association at 25 °C and dissociation at 50 °C (Table S2, Supporting Information). The equilibrium constants are concluded to follow the order $(TA)_{14:7} \gg (TA)_7{}^{cc} > \mathbf{X} = (TA)_7 > (TA)_{8:7} \gg \mathbf{X} = (TA)_5$, where the ratio for $(TA)_{14:7}$ and $\mathbf{X} = (TA)_5$ exceeds 3 orders of magnitude. Evidently, the presence of unpaired regions in DNA can largely influence the free energy of the transition state and the final threaded state.

In conclusion, we have shown that, above a threshold AT tract length corresponding to one turn of the B-DNA helix, the threading rate of four binuclear Ru complexes is increased by 2 orders of magnitude. In terms of association kinetics, the critical length interval of 10−14 AT base pairs spans the previously reported great "rate leap" between long AT DNA and mixed-sequence DNA. We present a hypothesis that a pre-equilibrium involving a conformational change in the DNA region around the binding site could account for the kinetic shift. The intercalation mechanism described above could lead to a DNA conformation that effectively resembles A-DNA. A-form DNA has a tighter major groove and an increased duplex diameter. The threaded state would thereby benefit from an increased electrostatic attraction between the phosphate backbone and the non-intercalated unit of the Ru complex (Figure 10).

DNA recognition is most commonly attained by direct targeting of a sequence of base pairs. Our findings show that, even for relatively simple molecules, additional selection can be found in the special character that a longer stretch of base pairs can confer to the double helix.

Acknowledgment. The project was founded by the The Swedish Research Council (VR) and the European Commission's Sixth Framework Programme (Project Reference AMNA, Contract No. 013575). F.W. acknowledges the Knut and Alice Wallenberg foundation for funding.

Supporting Information Available: Association kinetics with hairpins $\mathbf{X} = (TA)_{16}$ and $(TA)_{22}$, binding ratio dependence, UV melting curves, tables of $t_{1/2}$ of association and HPLC purification, capillary electrophoresis, and mass spectra analysis of functionalized hairpins. This material is available free of charge via the Internet at http://pubs.acs.org.

JA804427Q